

Received May 13, 2017; reviewed; accepted September 2, 2017

Trace muscovite dissolution separation from vein quartz by elevated temperature and pressure acid leaching using sulphuric acid and ammonia chloride solutions

Min Lin, Zhen-Yu Pei, Shao-Min Lei, Yuan-Yuan Liu, Zhang-Jie Xia, Fei-Xiang Xie

School of Resources and Environmental Engineering, Wuhan University of Technology, 430070, Wuhan, China

Corresponding author: 13297013624@163.com (Min Lin)

Abstract: Effects of sulphuric acid and ammonia chloride on muscovite dissolution were studied in acid leaching of vein quartz under elevated temperature and pressure. The leaching processes have been studied in detail by analyzing sources of impurity minerals, optimizing leaching process, analyzing leaching kinetics of Al in muscovite and charactering leaching mechanism of muscovite. The results showed that elements of Al and K mainly occurred in muscovite, and 98.10% or more of muscovite could be removed by acid leaching, while the process had limited influence on the particle size of quartz sand. Leaching of Al in the quartz ore was mainly controlled by chemical reaction. A calcination process and ammonia chloride were used for reducing chemical reaction resistance by damaging crystal structure of muscovite and providing stable acid leaching environment. Combined with the calcination process, muscovite, as a main gangue mineral, was effectively extracted during acid leaching of vein quartz at elevated temperature and pressure.

Keywords: vein quartz, muscovite, sulphuric acid, ammonium chloride, acid leaching

1. Introduction

Vein quartz, as an industrial substitute of crystal, usually contain some muscovite (Nie et al., 2013), and many major deposits are contaminated by small amounts of Al (200-400 ppm). Thus removal of muscovite minerals from quartz ore is one of the most important issues, and particularly attracts interest from producers of such industrial minerals. The quartz processing technologies such as flotation and acid leaching have been fully developed (Veglió et al., 1998; Wang et al., 2014). Fluorides were widely used in these technologies because of their distinctive destructiveness to silicon-oxygen structure (Larsen and Kleiv, 2016). Fluoric reagents, especially hydrofluoric acid, may seriously pollute environment (Dasgupta, 1998; An et al., 2015), although they can effectively remove aluminosilicate minerals from quartz ore (Caldwell, 1999).

It is noted that only quartz sand with specific particle sizes could be regarded as industrial mineral (Lassiter, 1990; Hu et al., 2007) because a certain accumulative porosity is needed during fused quartz preparation. Therefore, the quartz ore cannot be grinded to be very fine for complete dissociation of muscovite and quartz. Although leaching techniques are more effective than flotation for removing impurities existed within intergrowths of quartz and muscovite (Zhou, 2005; Wu et al., 2015), the selectivity of HF acid leaching is very low, and the size of quartz sand would be sharply reduced as the impurities being removed (Knotter, 2000; Ying et al., 2004). Elevated temperature and pressure acid leaching with mixed agents consisting of acid and inorganic salt is believed to be an effective method to dissolve muscovite without the utilization of any fluorides (Xue et al., 2017). Metallic ion in the inorganic salt commonly is forbidden in quartz purification because it would unavoidably introduce metallic impurities, however NH_4Cl could theoretically avoid this problem.

The objective of this study is to elaborate effects of sulphuric acid and ammonium chloride on removing of muscovite from quartz ore via acid leaching at elevated temperature and pressure. The

research is focused on mineralogical study of quartz, optimizing leaching process, analyzing leaching kinetics of Al in muscovite and charactering calcination and leaching mechanisms of muscovite.

2. Materials and methods

2.1 Materials

The quartz rock and quartz sand are from Qichun County of Hubei Province. The contents of main metallic elements in the quartz ore were analyzed by Inductively Coupled Plasma Spectrometer-Optical Emission Spectr (ICP-OES, Prodigy 7). As shown in Table 1, main metallic elements in quartz are Al (352.7 $\mu\text{g/g}$), K (118.1 $\mu\text{g/g}$) and Fe (61.22 $\mu\text{g/g}$). The particle size and specific area of quartz sand were analyzed by Laser Granulometer (BT9300S), the analysis result is shown in Fig. 1 while 88.25% of quartz sand is larger than 100 μm .

Table 1. Contents of main metallic elements for Qichun sample

Element	Fe	Li	Mg	Mn	Ti	Ca	K	Na	Al	In total
Content ($\mu\text{g/g}$)	61.22	2.201	11.81	0.9226	8.341	8.054	118.1	13.45	352.7	576.80

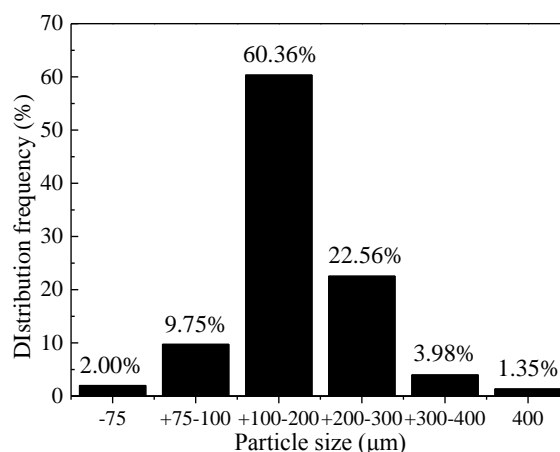


Fig. 1. Particle size distribution of quartz sand

2.2 Methods

2.2.1 Sample preparation

Quartz rock was sliced and the cross section was polished for microscopic examination. Quartz sand was calcined at 1173.15 K for 5 h in muffle furnace (KSY-12-16A). The calcined quartz sand was poured into ultrapure water (18.25 $\text{M}\Omega\text{ cm}$) in order to cooled to room temperature rapidly, and then dried for the experiments.

2.2.2 Mineralogical study

The quartz cross sections were observed by polarizing microscope (DLMP) to investigate gangue minerals. Calcined quartz sand was used for leaching experiment and analyzing morphology, and the composition of associated minerals by scanning electron microscope (JSM-5610LV) and electron probe (JXA-8230/INCA-ACT).

2.2.3 Acid leaching at elevated temperature and pressure

All leaching experiments were conducted in a reaction kettle with lining of para polystyrene (PPL, 100 cm^3). The experimental apparatus was shown in Fig. 2. The reaction temperature was controlled by electrothermal air blow drying cabinet (DHG-9075A). Pressure was autogeneous and was controlled by temperature in the airtight leaching system. In general, the liquid/solid ratio was 5 cm^3/g (10 g of mineral and 50 cm^3 of mixed acid and salt solutions), and leaching time was 7 h. Single factor tests

with respect to reaction temperature with or without NH_4Cl , H_2SO_4 concentration at different temperatures, and $c(\text{NH}_4\text{Cl})/c(\text{H}_2\text{SO}_4)$ ratio were carried out. Leached quartz sand was washed for 5-10 times with ultrapure water, and then dried in electrothermal air blow drying cabinet. The quartz sand samples were treated by HF for analyzing metallic element content by ICP-OES, while contents of metal elements in quartz concentrate were also examined by ICP-MS (Thermo ICAP Qc).

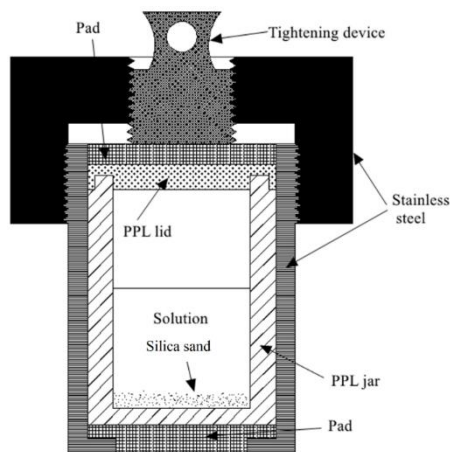


Fig. 2. Experimental apparatus

The optimum muscovite removal effect was approximately evaluated by calculating extraction yield of K in quartz concentrate although few removed K was from quartz lattice (Götze et al., 2004). However, it was best to use the extraction yield of Al to evaluate muscovite removal effect in single factor tests because K in interlayer was usually leached prior to Al in layered silicate mineral. In this case:

$$\eta = \eta(\text{K}),$$

where η is the optimum muscovite removal yield, and $\eta(\text{K})$ is the K extraction yield of under optimum leaching condition.

The leaching kinetics of removing Al from quartz sand was studied at different leaching temperature. Based on this, apparent activation energy of pressure acid leaching was calculated:

$$\ln k = -\frac{E_a}{RT} + \ln A,$$

where T is leaching temperature, k is rate constant of action at different temperature, R is molar gas constant (8.314 J/(mol·K)), E_a is apparent activation energy, and A is pre-exponential factor.

Referenced and suitable kinetics models of muscovite dissolution including shrinking core model and Avrami model are as follows (Avrami, 1939; Tan et al., 1996; Dietzel, 2000; Zhong et al., 2015):

1) Shrinking core model: chemical reaction control: $1-(1-x)^{1/3}=kt$; internal diffusion control: $1-2x/3-(1-x)^{2/3}=kt$, where x is reaction fraction, k is comprehensive rate constant of action at different temperature, and t is leaching time.

2) Avrami model: $\ln(-\ln(1-x))=n\ln t + \ln k$, where n is grain parameter that is relative to reaction mechanism.

3. Results and discussion

3.1 Mineral impurities in quartz

As shown in Fig. 3, gangue minerals including muscovite, secondary hematite and kaolinite were observed by polarizing microscope. The muscovite and secondary hematite widely occurs in the quartz, but the proportion of kaolinite is negligible. As shown in Fig. 4 and Table 2, the muscovite in calcined quartz sand contains some metallic elements such as Al (wt 16.15%), K (wt 8.74%), Fe (wt 3.80%), Mg (wt 1.09%) and Ti (wt 0.47%). Combined with microscopic analyses and content analyses of the metallic elements (Table 1), it is indicated that elements Al and K mainly occurs in muscovite. So their contents in quartz sand can be used to evaluate the content of trace muscovite.

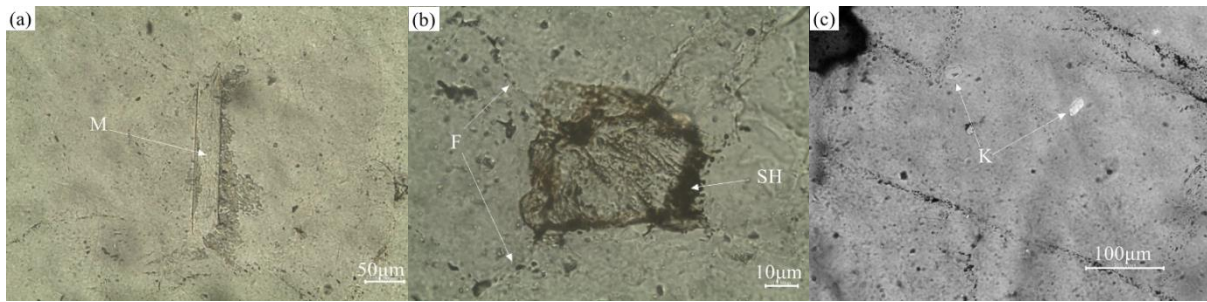


Fig. 3. Associated minerals in quartz sections by polarizing microscope (transmission light): (a) M-muscovite, (b) SH-secondary hematite in quartz fracture (F), (c) K-kaolinite

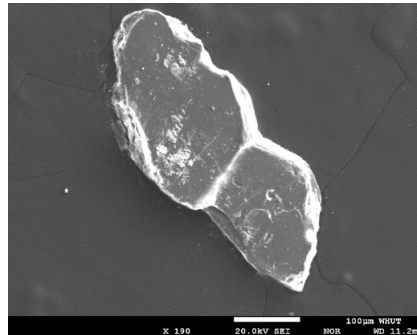


Fig. 4. Secondary electron image (SEI) of muscovite from calcined quartz sand

Table 2. Contents of main elements of muscovite from calcined quartz sand (wt.%)

Element	Si	O	Al	K	Fe	Mg	Ti	In total
Content	24.07	45.69	16.15	8.74	3.80	1.09	0.47	100.00

3.2 Effect of leaching temperature on muscovite dissolution

Element Al in quartz sand was removed by dissolving muscovite in NH_4Cl and H_2SO_4 acid leaching system at elevated temperature and pressure. Extraction yields of Al (M_i , N_i) with or without NH_4Cl were used to determine critical temperature at which NH_4Cl began to promote leaching reaction:

$D = M_i - N_i$, $i = 423.15, 433.15, 443.15, 453.15, 463.15, 473.15, 483.15, 493.15, 503.15, 513.15$ and 523.15 K where M_i is extraction yield of Al with $100 \text{ mmol/dm}^3 \text{ H}_2\text{SO}_4 + 200 \text{ mmol/dm}^3 \text{ NH}_4\text{Cl}$, and N_i is extraction yield of Al with $100 \text{ mmol/dm}^3 \text{ H}_2\text{SO}_4$.

Fig. 5 showed that an obvious turning point occurred at 453.15 K at which NH_4Cl began to accelerate leaching reaction. The negative effect of NH_4Cl was reversed around 463.15 K and then actually promoted Al extraction with further increasing of leaching temperature. So NH_4Cl promoted the muscovite removal at 463.15 K or above.

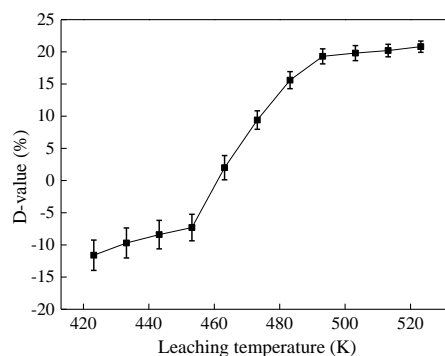


Fig. 5. Effect of leaching temperature on the values of D: leaching time 3 h, NH_4Cl 100 mmol/dm^3 , $c(\text{NH}_4\text{Cl})/c(\text{H}_2\text{SO}_4)$ ratio=2

3.3 Effect of agent consumption on muscovite dissolution

The results of single factor tests about H_2SO_4 concentration at different temperatures are shown in Fig. 6. Extraction yields of Al increased with the H_2SO_4 concentration at 423.15, 473.15 and 523.15 K. At 523.15 K, the extraction yield reached 86.1% with H_2SO_4 of 300 mmol/dm^3 , but slightly decreased right afterwards. The higher the temperature, the greater the extraction yield with the same H_2SO_4 concentration. So leaching temperature of 523.15 K and H_2SO_4 concentration of 300 mmol/dm^3 were adopted for following experiment.

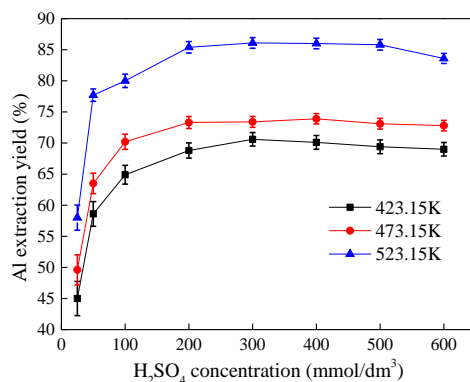


Fig. 6. Effect of H_2SO_4 concentration on Al extraction yield: L/S ratio-5 cm^3/g , leaching time 7 h, $c(\text{NH}_4\text{Cl})/c(\text{H}_2\text{SO}_4)$ ratio=2

3.4 Effect of agent ratio on muscovite dissolution

Fig. 7 shows that extraction yield curve of Al had two humps when $c(\text{NH}_4\text{Cl})/c(\text{H}_2\text{SO}_4)$ ratio was 1.5 and 3.5, respectively. Apparently, agent ratio of 1.5 was better than 3.5 because it consumed less NH_4Cl . And the extraction yield of Al reached 87.5% at agent ratio of 1.5. The NH_4Cl promoted the extraction of Al at $c(\text{NH}_4\text{Cl})/c(\text{H}_2\text{SO}_4)$ ratio of 1.5, but NH_4^+ may reduce H^+ and muscovite contact probability with further increasing of $c(\text{NH}_4\text{Cl})/c(\text{H}_2\text{SO}_4)$ ratio (especially at 2.5). The second hump indicated that NH_4Cl was the host leaching agent when $c(\text{NH}_4\text{Cl})/c(\text{H}_2\text{SO}_4)$ ratios ranging from 3.0 to 4.0.

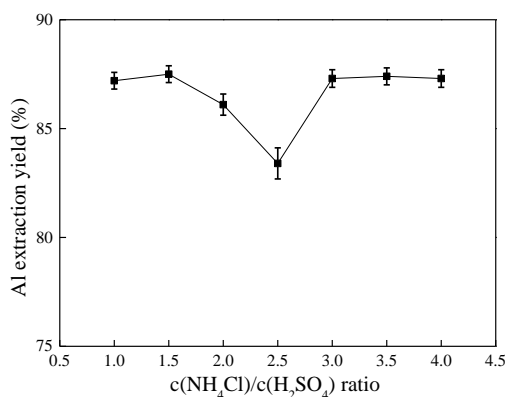


Fig. 7. Effect of $c(\text{NH}_4\text{Cl})/c(\text{H}_2\text{SO}_4)$ ratio on Al extraction yield: L/S ratio 5 cm^3/g , reaction time 7 h, H_2SO_4 300 mmol/dm^3 , leaching temperature 523.15 K

3.5 Effect of elevated temperature and pressure on muscovite dissolution

The contents of main metallic elements in quartz ore and leached quartz sand were shown in Table 3. The total content of main metal elements was reduced from 576.80 $\mu\text{g}/\text{g}$ to 79.135 $\mu\text{g}/\text{g}$ while total extraction yield reached 86.3%. In addition, elements Al, K and Fe could be effectively removed with a certain removals of elements Mg, Mn, Ti and Ca. Extraction yields of Li and Na was lower due to their

different existence states (Botis and Pan, 2009). The optimum removal effect of muscovite: $\eta = \eta(K) = \frac{118.1 - 2.241}{118.1} = 98.10\%$ under optimum leaching conditions listed in Table 4.

Table 3. Main metallic element contents in quartz ore and leached quartz

Elements	Fe	Li	Mg	Mn	Ti	Ca	K	Na	Al	In total
Ore	61.22	2.201	11.81	0.9226	8.341	8.054	118.1	13.45	352.7	576.80
Concentrate ($\mu\text{g/g}$)	1.123	2.038	7.146	0.5350	5.376	4.396	2.241	12.19	44.09	79.135

Table 4. Optimum conditions about leaching process

Factor	H ₂ SO ₄ (98%)	NH ₄ Cl	Reaction time	L/S Ratio	Temperature
Condition	0.3 mol/dm ³	0.45 mol/dm ³	7 h	5 cm ³ /g	523.15K

3.6 Effects of calcination on quartz acid leaching

Combining calcination and elevated temperature and pressure acid leaching, intergrowth and inclusion impurities in quartz were removed. As shown in Fig. 8(a), adherent gangue mineral was separated from quartz due to their different thermal expansibilities during calcination. Because gangue impurities lead to a rough surface of calcined quartz, the surface of leached quartz (Fig. 8(b)) was smoother than that of calcined quartz (Fig. 8(a)). This observation indicated that intergrowth impurities were separated from quartz particle during calcination and then dissolved by elevated temperature and pressure acid leaching. Inclusion impurities inside quartz were exposed to leaching agents due to thermal expansibility during calcination. As shown in Fig. 8(c), fracture on the surface of quartz was caused by heat stress. Different thermal expansibilities of quartz and its inclusions provided a way to remove the inclusions although the process commonly increased superficial area of quartz sand.

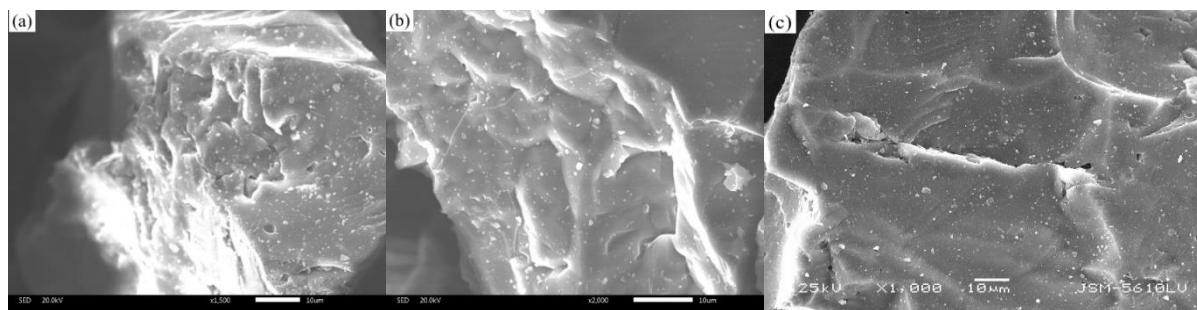


Fig. 8. SEIs of quartz particles: (a)-rough surface of calcined quartz particle (1173.15K for 5 h), (b)-smooth surface of quartz sand leached at the best conditions, (c)-fracture on surface of calcined quartz particle (1173.15 K for 5 h)

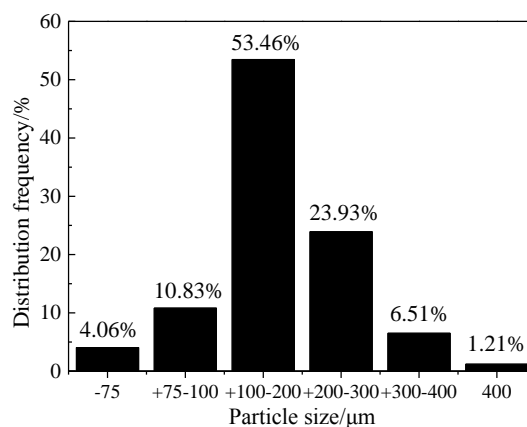


Fig. 9. Particle size distribution of quartz leached at the best conditions

As shown in Fig. 9, 85.11% of particles in quartz concentrate was larger than 100 μm . There was only 3.56% reduction relative to the quartz sand ore. Meanwhile, the specific area (Table 5) of quartz increased from 14.99 m^2/kg to 16.94 m^2/kg , and the tiny increasing rate of 13.01% indicated that this process without HF had limited influence on particle size of quartz, indicating that some fractures occurred in quartz particle due to the removal of inclusion mineral. The result was consistent with Fig. 8(c).

Table 5. Specific areas of quartz at different periods

Specific area / m^2/Kg		
Ore	Sample after calcination	Concentrate
14.99	15.09	16.94

3.7 Leaching kinetics of element Al

As shown in Fig. 10(a), the leaching kinetics of element Al was carried out with 0.3 mol/dm^3 H_2SO_4 and 0.45 mol/dm^3 NH_4Cl at different leaching temperatures while the leaching liquid/solid ratio was 5 cm^3/g . Avrami model and shrinking core model are shown in Table 6 according to coefficient of determination (R^2), although external diffusion control of shrinking core model is not shown due to low R^2 . The Avrami model was more suitable than shrinking core model according to the correlation coefficient. In the fitting of shrinking core model, internal diffusion control was more important than chemical reaction control. It indicated that the leaching process was mainly limited by the diffusion of leaching agents from leaching liquid to the core of muscovite. Zhong (2015) reported that leaching reaction was controlled by chemical reaction and internal diffusion when n ranges from 0.5 to 1.0, but only by diffusion process when n was less than 0.5. In the fitting of Avrami model, n was always more than 0.5 but less than 1.0 while the n decreased with leaching temperature. It indicated that the leaching process was jointly influenced by chemical reaction and internal diffusion. With the leaching temperature, the influence of chemical resistance decreased, and diffusion resistance increased. Based on the fitting of Avrami model, apparent activation energy of leaching Al from quartz sand was 52.18 kJ/mol according to Fig. 10(b). So the leaching process of element Al was mainly controlled by chemical reaction.

In summary, reducing of muscovite particle size and increasing of leaching temperature are effective methods to reduce chemical reaction resistance. As mentioned in the introduction, grinding is inadvisable because of the special demanding for particle size in quartz processing. Calcination, as a retreatment technology to activate muscovite by reducing its size and increasing possible fractures, is effective for promoting the dissolution separation of muscovite from vein quartz sand.

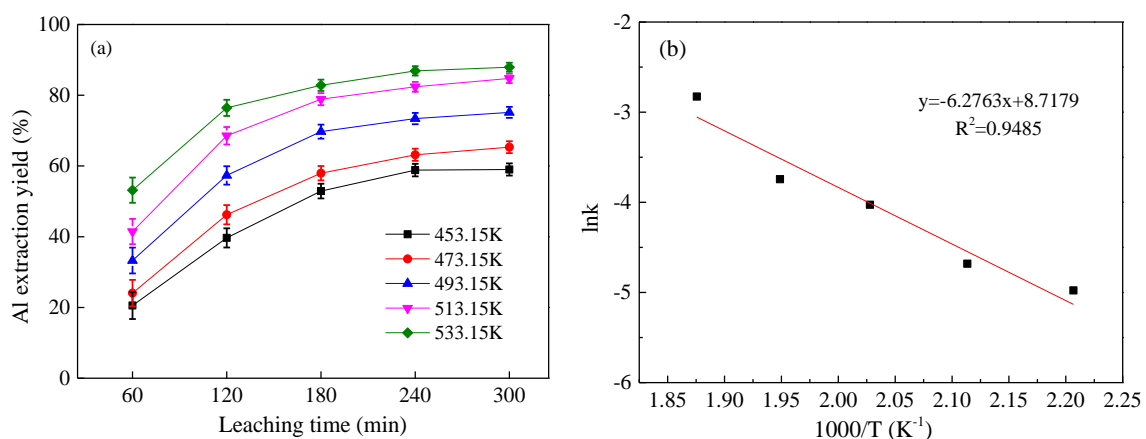


Fig. 10. Leaching kinetics and apparent activation energy curve of acid leaching

Table 6. Leaching control models of element Al

Leaching control model	Leaching temperature (K)	Regression equation	R ²	k
Chemical reaction control	453.15	$1-(1-x)^{1/3}=0.0008t$	0.8900	0.0007795
	473.15	$1-(1-x)^{1/3}=0.0009t$	0.9006	0.0008597
	493.15	$1-(1-x)^{1/3}=0.0010t$	0.8745	0.0099996
	513.15	$1-(1-x)^{1/3}=0.0012t$	0.8784	0.0012071
	533.15	$1-(1-x)^{1/3}=0.0011t$	0.8641	0.0011242
Shrinking core model	453.15	$1-2x/3-(1-x)^{2/3}=0.0002t$	0.9253	0.0002201
	473.15	$1-2x/3-(1-x)^{2/3}=0.0003t$	0.9480	0.0002697
	493.15	$1-2x/3-(1-x)^{2/3}=0.0004t$	0.9142	0.0003739
	513.15	$1-2x/3-(1-x)^{2/3}=0.0005t$	0.9151	0.0005127
	533.15	$1-2x/3-(1-x)^{2/3}=0.0005t$	0.8892	0.0005133
Avrami model	453.15	$\ln(-\ln(1-x))=0.8797\ln t-4.9778$	0.9566	0.0068892
	473.15	$\ln(-\ln(1-x))=0.8530\ln t-4.6804$	0.9572	0.0092753
	493.15	$\ln(-\ln(1-x))=0.7862\ln t-4.0266$	0.9516	0.0178349
	513.15	$\ln(-\ln(1-x))=0.7865\ln t-3.7439$	0.9540	0.0236616
	533.15	$\ln(-\ln(1-x))=0.6434\ln t-2.8274$	0.9545	0.0591665

3.8 Calcination and leaching mechanisms

Calcination promoted stratification of muscovite and structure damage. As shown in Fig. 11(a), surface layer of muscovite exfoliated from its host. With the calcination, the exfoliated muscovite sheet was further damaged into active fragment, as shown in Fig. 11(b). The effects of calcination on muscovite were propitious to muscovite dissolution in subsequent elevated temperature and pressure acid leaching.

Changes of muscovite during calcination (1173.15 K for 5 h) could be divided into three stages (Zhu et al., 2008; Liu and Lin, 2008; Shan et al., 2013):

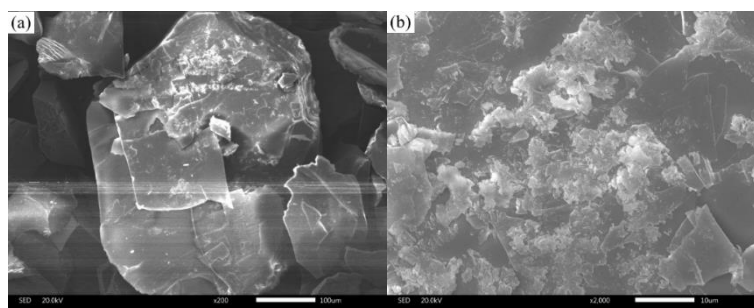
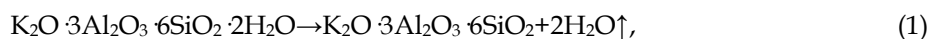
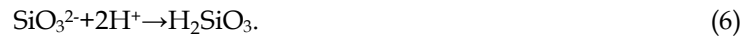
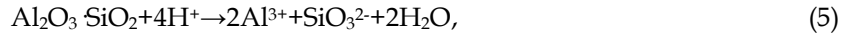


Fig. 11. SEIs of muscovite in calcined quartz sand: (a)-surface topography of muscovite, (b)-active fragments on surface of muscovite

First, planar water and constitution water were removed from muscovite, and the evaporation of these water increased interlayer spacing of muscovite. The crystal structure of this muscovite changed due to calcination, and then the active Al_2O_3 and SiO_2 formed. Finally, some active Al_2O_3 reacted with SiO_2 to form another stable phase, such as andalusite (Liu and Lin, 2008). This stable phase on the edge of muscovite stopped further migration of Al to quartz particle. And some fractures occurred in calcined muscovite. These activation effects reduced chemical reaction resistance of dissolving muscovite. Active Al_2O_3 and the stable phase could be dissolved with leaching agent.





As shown in Fig. 12, active SiO_2 and the stable phase were reacted with H^+ from H_2SO_4 to form H_2SiO_3 in the form of colloid which was strongly attracted to the surface A for hindering the further reaction.

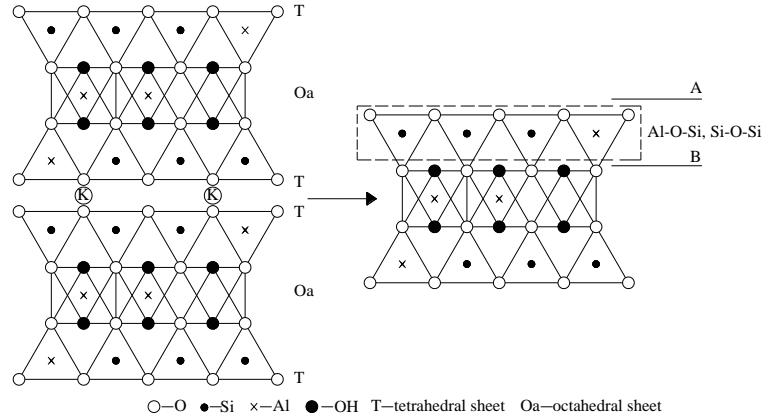
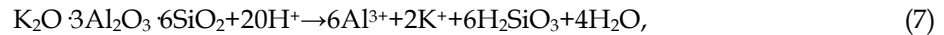


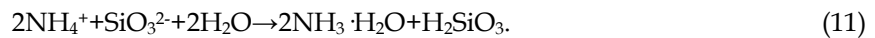
Fig. 12. Image of muscovite crystal structure (Jackson and West, 2015; Comodi and Zanazzi, 1995)

Most of Al-O-Si and Si-O-Si of muscovite were damaged by H^+ . And then Al^{3+} , a product of reaction (7), might be triggered to hydrolyze at elevated temperature (reaction (8)) and Si-O structure (reaction (9)) in close layer (Gao et al., 1993; Hou et al., 2016) when the H^+ was consumed in large quantities.



This colloid consisting of $\text{Al}(\text{OH})_3$ and H_2SiO_3 from reaction (9) was accumulated on surface B so that it could hinder damage of dioctahedron and dissolution of Al by reducing contact probability of dioctahedron and H^+ . The special colloid hindered the diffusion of leaching agents from leaching liquid to core of muscovite, and then hindered the leaching reaction (Zhong, 2015). The result is consistent with the finding of increased diffusion resistance in leaching kinetics of element Al.

NH_4^+ could react with silicon oxygen structure (Yang et al., 2016) so as to avoid producing excessive amounts of $\text{Al}(\text{OH})_3$ in a short period of time (reaction (11)):



Positively charged NH_4^+ could be adsorbed on the growing H_2SiO_3 colloid surface, which is negatively charged, thus hindering its further growth. By this way, NH_4^+ reduced the resistances from chemical reaction and internal diffusion.

Because the H_2SO_4 almost completely ionized in leaching solution:



the concentration of H^+ in leaching system with only H_2SO_4 decreased with the leaching reaction. But NH_4^+ could provide more stable leaching environment due to hydrolysis. With the consuming of H^+ , the hydrolysis balance of NH_4^+ moved to right for maintaining the concentration of H^+ so as to reduce chemical reaction resistance due to concentration decreasing of leaching agents:



At the same time, the H^+ from reaction (13) could dissolve potential $\text{Al}(\text{OH})_3$ from reactions (8) and (9) in turn. More accurately, the NH_4^+ inhibited the hydrolysis of Al^{3+} in hydrated layer.

Furthermore, the influence of Cl⁻ on the leaching of Al³⁺, especially for dissolution process, cannot be ignored (Lee et al., 2009). Solubility of metal chlorides including AlCl₃, FeCl₃, CaCl₂ and TiCl₄ are generally higher than that of their sulfates. Thus, the Cl⁻ from NH₄Cl ionization could promote dissolution of metal impurities.

The main effect of calcination process was to destroy crystal structure of muscovite. The damaged muscovite was effectively dissolved by mixed leaching agents consisting of H₂SO₄ and NH₄Cl. In addition, the H₂SO₄ only provided H⁺, and the NH₄Cl maintained its concentration during leaching process. In addition, the NH₄Cl inhibited the hydrolysis of Al³⁺ at elevated temperature (reaction (8)) and Si-O structure (reaction (9)), and further promoted dissolution of Al by introducing Cl⁻.

The muscovite dissolution mechanisms are also suitable for explaining the removal of kaolinite because of their similar crystal structure. Moreover, hematite as main iron-bearing gangue mineral was efficiently removed according to Table 3. Stable leaching environment and high leaching temperature were also propitious to dissolve hematite:



In summary, the process could realize a high-efficiency purification of vein quartz via calcination and acid leaching at elevated temperature and pressure without addition of any fluorides.

4. Conclusions

(1) Mineralogical study showed that the main gangue minerals in the quartz were muscovite, hematite and kaolinite, and the muscovite was the main source of elements Al and K.

(2) Elevated temperature and pressure acid leaching experiment showed that the contents of Al and K in vein quartz were reduced to 44.09 µg/g and 2.241 µg/g, respectively, when the quartz was leached at 523.15K for 7 h with 5 cm³/g, using leaching agent consisting of 0.30 mol/dm³ H₂SO₄ and 0.45 mol/dm³ NH₄Cl. 98.10% or more muscovite was removed under optimum leaching conditions while the leaching using H₂SO₄ and NH₄Cl had limited influence on the particle size of quartz sand.

(3) Leaching kinetics study of element Al with respect to leaching temperature showed that the element Al leaching process in quartz ore was mainly controlled by chemical reaction, and the apparent activation energy of leaching reaction reached 52.18 kJ/mol.

(4) Muscovite was damaged by calcination process, and then effectively dissolved by fluorine-free leaching system. The ammonia chloride was hydrolyzed to provide stable acid leaching environment and inhibited the hydrolysis of Al³⁺ at elevated temperature. Combined with the two effects on reducing chemical reaction resistance, elements Al in muscovite could be effectively leached out from vein quartz sand using elevated temperature and pressure acid leaching method.

Acknowledgements

This research was supported by the Open Foundation of Engineering Center of Avionics Electrical and Information Network of Guizhou Province Colleges and Universities (HKDZ201404). Special thanks to Prof. Changqi Peng for guidance in mineralogy analysis.

References

- AN J., LEE H.A., LEE J., YOON H.O., 2015. Fluorine distribution in soil in the vicinity of an accidental spillage of hydrofluoric acid in Korea. *Chemosphere*, 119C, 577-582.
- AVRAMI M., 1939. *Kinetics of Phase Change. I General Theory*. *J. Chem. Phys.*, 7, 1103-1112.
- BOTIS S.M., PAN Y., 2009. Theoretical calculations of [AlO₄/M⁺]⁰ defects in quartz and crystal-chemical controls on the uptake of Al. *Mineral. Mag.*, 73, 537-550.
- CALDWELL R.W., 1999. *Methods and apparatus for screening particulate materials*. US, US 5992641A.
- COMODI P., ZANAZZI P.F., 1995. High-pressure structural study of muscovite. *Phys. Chem. Miner.*, 22, 170-177.
- DASGUPTA P. K., 1998. Comment on "hydrofluoric acid in the Southern California atmosphere". *Environ. Sci. Technol.*, 31, 427.
- DIETZEL M., 2000. Dissolution of silicates and the stability of polysilicic acid. *Geochim. Cosmochim. Acta*, 64, 3275-3281.

- GAO B.Y., LI C.P., YUE Q.Y., AI Z.P., WANG S.R., 1993. *Interaction between aluminum ion with poly silicic acid*. Environ. Chem., 12, 268-273.
- GOTZE J., PLOTZE M., GRAUPNER T., HALLBAUER D.K., BRAY C.J., 2004. *Trace element incorporation into quartz: a combined study by ICP-MS, electron spin resonance, cathodoluminescence, capillary ion analysis, and gas chromatography 1*. Geochim. Cosmochim. Acta, 68, 3741-3759.
- HOU X.X., DONG S.N., Zhang J., SHU-PING B.I., 2016. *DFT study of the static structural and ^{27}Al -/ ^{17}O -/ ^1H -NMR characteristics for the third hydration shell of Al^{3+} (aq) complexes*. J. Anal. Sci., 32, 149-155.
- HU X.Q., LI G.L., SUN M., CHAO H.H.. *Study on controlling of the crystal form and the size distribution on the silica sands being used for material of the quartz glass*. China Non-Met. Min. Ind. Her., 4, 41-43.
- JACKSON W.W., WEST J., 2015. *The crystal structure of muscovite- $\text{KAl}_2(\text{AlSi}_3\text{O}_{10})(\text{OH})_2$* . Z. Krist.-Cryst. Mater., 85, 160-164.
- KNOTTER D.M., 2000. *Etching mechanism of vitreous silicon dioxide in HF-Based solutions*. J. Am. Chem. Soc., 122, 4345-4351.
- LARSEN E., KLEIV R.A., 2016. *Flotation of quartz from quartz-feldspar mixtures by the HF method*. Miner. Eng., 98, 49-51.
- LASSITER P.B., 1990. *Method of manufacturing cast fused silica articles*. US, US 4929579 A.
- LEE K.Y., YOON Y.Y., JEONG S.B., CHAE Y.B., KO K.S., 2009. *Acid leaching purification and neutron activation analysis of high purity silicas*. J. Radioanal. Nucl. Chem., 282, 629-633.
- LIU C., LIN J.H., 2008. *Influence of calcination temperature on dielectric constant and structure of the micro-crystalline muscovite*. China Non-Met. Min. Ind. Her., 5, 37-39.
- NIE Y.M., LU X.L., NIU F.S., 2013. *Purification experiment research of quartz sand*. Appl. Mech. Mater., 389, 346-348.
- SHAN Z.Q., SHU X.Q., FENG J.F., ZHOU W.N., 2013. *Modified calcination conditions of rare alkali metal Rb-containing muscovite ($\text{KAl}_2[\text{AlSi}_3\text{O}_{10}](\text{OH})_2$)*. Rare Metals, 32, 632-635.
- TAN K., ZHANG Z., WANG Z., 1996. *The mechanism of surface chemical kinetics of dissolution of minerals*. Acta Geochim., 15, 51-60.
- VEGLIO F., PASSARIELLO B., BARBARO M., PLESCIA P., MARABINI A.M., 1998. *Drum leaching tests in iron removal from quartz using oxalic and sulphuric acids*. Int. J. Miner. Process., 54, 183-200.
- WANG L., SUN W., HU Y.H., XU L.H., 2014. *Adsorption mechanism of mixed anionic/cationic collectors in muscovite-quartz flotation system*. Miner. Eng., 64, 44-50.
- WU X., SUN H.J., PENG T.J., XIAN H.Y., LA J.D., MA J.H., 2015. *Process mineralogy study and beneficiation test of a vein quartz ore from Qinghai province*. Min. and Metall., 24, 71-77.
- XUE N.N., ZHANG Y.M., LIU T., HUANG J., ZHENG Q.S., 2017. *Effects of hydration and hardening of calcium sulfate on muscovite dissolution during pressure acid leaching of black shale*. J. Clean Prod., 149, 989-998.
- YANG S.H., HAO L.I., SUN Y.W., CHEN Y.M., TANG C.B., JING H.E., 2016. *Leaching kinetics of zinc silicate in ammonium chloride solution*. Trans. Nonferrous Met. Soc. China, 26, 1688-1695.
- YING S.U., ZHOU Y., HUANG W., ZHENAN G.U., 2004. *Study on reaction kinetics between silica glasses and hydrofluoric acid*. J. Chin. Ceram. Soc., 32, 287-293.
- ZHONG L.L., 2015. *Study on purification and mechanism of ultra-high purity quartz sand*. PhD Thesis, Wuhan University of Technology.
- ZHOU Y.H., 2005. *Study on refining quartz powder by leaching in HF acid solution*. J. Mineral. Petrol., 25, 23-26.
- ZHU B.Z., SUN Y.L., XIE C.W., 2008. *Spectroscopy research on the Guizhou Xingyi gangue of different calcined temperatures*. J. China Coal Soc., 33, 1049-1052.